

# Diagnosis of a Combined Alkali Silica Reaction and Delayed Ettringite Formation

Lalita Baingam<sup>1</sup>, Warangkana Saengsoy<sup>2</sup>, Pongsak Choktaweekarn<sup>2</sup> and Somnuk Tangtermsirikul<sup>1</sup>

<sup>1</sup> School of Civil Engineering and Technology, Sirindhorn International Institute of Technology (SIIT), Thammasat University, Pathum Thani, Thailand.

<sup>2</sup> Construction and Maintenance Technology Research Center, Sirindhorn International Institute of Technology, Thammasat University, Pathum Thani, Thailand.

## Correspondence:

Lalita Baingam

School of Civil Engineering and Technology, Sirindhorn International Institute of Technology, Thammasat University, Pathum Thani, Thailand  
E-mail: lalita\_baingam@hotmail.com

## Abstract

*This paper presents a case study of diagnosing alkali silica reaction (ASR) and delayed ettringite formation (DEF) in mass concrete structures in order to identify causes of cracks in the concrete. In the investigation, cored concrete samples were taken from real concrete structures with 4 different levels of damage identified by none, moderate, severe, and very severe. Microscopic examinations were conducted to identify ettringite formation and ASR products in the concrete. Results revealed that the ettringite and ASR products were found in many locations of all concrete samples and their amounts were consistent with the damage levels of the concrete structures. Moreover, the semi-adiabatic temperature rise in these concrete structures was analyzed by using the authors' heat model and finite element method (FEM). It was found that the temperature rise of the concrete was above 70°C, supporting the possible occurrence of DEF. From the results, it can be concluded that ASR and DEF are two of the mechanisms that contribute to cracking of concrete structures. The formation of ettringite was considered to be not involved with the external sulfate attack. This can be considered as the first evidence of a combined case of ASR and DEF in Thailand.*

**Keywords:** alkali silica reaction (ASR), delayed ettringite formation (DEF), microscopic examination, semi-adiabatic temperature rise

## 1. Introduction

The concrete structures investigated in this study were constructed in 1998. Cracks in the concrete were observed in many locations within a few years after completion of the construction. The cracks were repaired by grouting with epoxy. However, recently inspection of those structures revealed that the repaired cracks were continuously extended and new cracks were formed. The damage levels varied from one structure to another and the cracking ranged from none to very severe. In order to arrange proper repair and maintenance planning of the concrete structures, causes of concrete deterioration are needed to be investigated.

Possible causes of cracks in concrete were investigated based on available data of construction records and visual inspection of several mass concrete structures. In general, cracking of a mass concrete structure can occur due to thermal effect and shrinkage. These kinds of crack can be repaired and their extensions can be controlled. In this case, cracks in the concrete still extended, even if they had been repaired.

According to onsite inspection, random cracks have been found on surfaces of the concrete structures as shown in Fig. 1. They are similar to the crack patterns due to alkali-silica reaction (ASR) and delayed ettringite formation (DEF). ASR and DEF may be two of the mechanisms that contribute to concrete expansion and cracking of these mass concrete structures.

ASR is a chemical reaction which occurs over time in concrete between the highly alkaline pore solution in the cement paste and the non-crystalline  $\text{SiO}_2$  in aggregates, producing alkali silica gel which can expand in the presence of moisture. The expanding gel causes cracks in the aggregates and in the paste, as well as high expansion, which can result in significant damage of concrete [1]. The investigation of ASR in concrete has been reported in research [1-7]. The possible signs of deteriorated concrete by ASR can be detected by the existence of efflorescence and exudation of ASR gel on concrete surfaces [2, 3].

It has been reported that ASR occasionally occurs together with DEF [4]. The signs of concrete deterioration due to ASR and DEF are quite similar, making it difficult to separate their individual contributions [7, 8].

DEF is one cause of concrete deterioration which induces concrete expansion. The expansion mechanism of this reaction is complex, and involves many parameters such as temperature, sulfate content in the mixtures, and the presence of moisture. At temperature above  $70^\circ\text{C}$ , this can lead to decomposition of ettringite to form monosulfate and sulfate. With a subsequent drop in temperature, the monosulfate becomes metastable. If there is sufficient moisture available, ettringite can be formed [5]. The formation of ettringite is frequently detected at the rim around aggregates and in air voids [6].

In order to diagnose ASR and DEF, it has been reported that microscopic examination is an effective mean to determine the characteristics of ASR and DEF products in concrete samples taken from real concrete structures. The microscopic examinations are such as Scanning electron microscopy with back-scatter electron mode (SEM/BSE), X-ray energy dispersive spectroscopy (EDX), and X-ray diffraction (XRD) analysis, etc [1-7].

The objective of this research is to investigate and to confirm whether the ASR and DEF are the causes of deterioration of the concrete structures. The full investigation involved an evaluation of a large number of concrete structures. The cored concrete samples extracted from four different damage levels of the concrete structures were taken for investigation in this study. The investigation includes microscopic examinations for identifying ASR and DEF products and simulation of the semi-adiabatic temperature rise of mass concrete to confirm the incidence of DEF. The content of sulfate in soils was also determined in order to verify the risk of external sulfate attack. Moreover, the residual expansion of the concrete cores was evaluated. The accomplishment of this study will be useful for managing proper repair and maintenance of those damaged concrete structures. This case can be considered as the first evidence of combined ASR and DEF in Thailand.

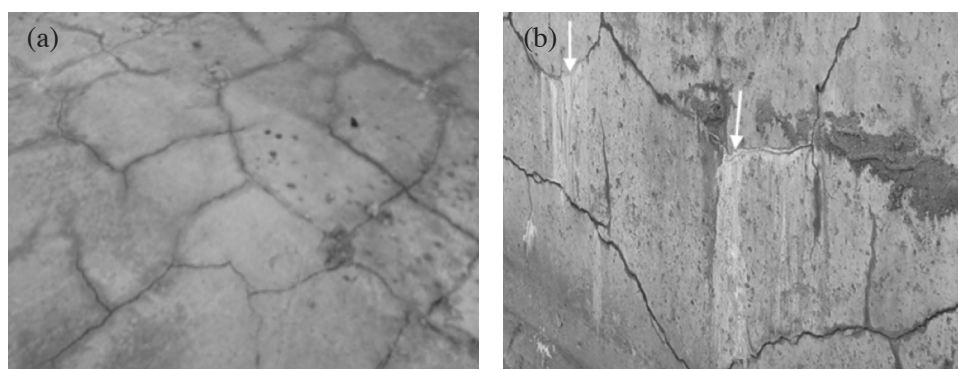


**Fig. 1.** Random cracks on surface of concrete structures (a) Opened cracks without exudation of ASR gel and (b) opened cracks with white translucent gel.

## 2. Details of concrete structures and cored concrete samples

The concrete structures investigated in this study were constructed in 1998. Dimension of each structure is 550 x 1330 x 250 cm. Since the structures are partly underground, visual inspection of the concrete above ground level has been primarily done. Based on the visual examination, damage of the concrete structures can be divided into 4 levels according to amount of cracks and crack width of the concrete structures, i.e., Very severe (A), Severe (B), Moderate (C), and None (D). The cored concrete samples extracted from the concrete structures having different damage levels were taken for investigation in this study.

The concrete cores with a dimension of 7 cm in diameter and 100 cm in length were separated for microscopic examination and residual expansion test as shown in Fig. 2. The microscopic examination was conducted on the cored concrete samples at the depths of 30 cm and 100 cm from the top surface to identify ASR and DEF products. The remaining part of the cored concrete samples at 30 to 100 cm deep was cut into two parts to measure the residual expansion of the concrete. Moreover, samples of soil near these concrete structures were taken to determine content of soluble-sulfate in soil according to ASTM C1580 in order to find the possibility of external sulfate attack. The soil samples were obtained at a depth of 100 cm below ground surface level, which is about the same level with the bottom faces of the structures.

## 3. Methodology

### 3.1 Residual expansion of cored concrete

Residual expansion test was conducted on concrete cores taken from the structures with 4 different levels of damage identified by Very severe (A), Severe (B), Moderate (C), and None (D). The cored samples were cut into 28.5 cm in length. Stainless steel studs were embedded in both ends of the cores. The cored concrete samples were submersed in a saturated lime solution at 40°C and measured for length change by using a length comparator at 3, 7, and 28 days. After 28 days, the measurements were made every month until the expansion of samples became stable [9]. The expansion of concrete for each damage level was obtained from the average of two cored specimens.

### 3.2 Scanning electron microscopy with back-scatter electron mode (SEM/ BSE) and x-ray energy dispersive spectroscopy (EDX) for investigating ASR products and ettringite

Samples were cut into a small size of 1×1×1 cm. The samples were mounted with epoxy resin and subsequently polished with sand papers (Nos. 120, 240, 400, 800, and 1200) and diamond powders (3 and 1 μm). The polished samples were coated with carbon before SEM analysis. SEM model JEOL JSM-6301F, equipped with an Oxford-INCA 350 energy dispersive spectrometer, was used. The accelerating voltage used was 20 kV.

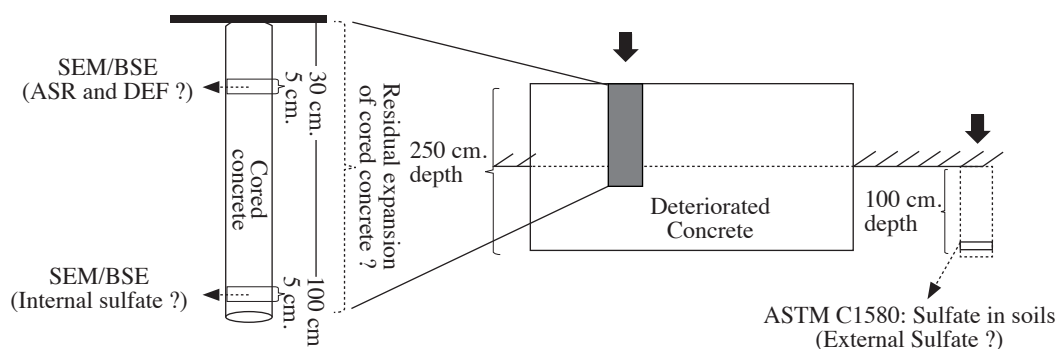


Fig. 2. Details of cored concrete.

### 3.3 Simulation of semi-adiabatic temperature rise of concrete

Since the temperature history of concrete during construction of the investigated structures was not available, semi-adiabatic temperature rise of the mass concrete was simulated.

A flow chart of the models for predicting semi-adiabatic temperature of mass concrete is shown in Fig. 3. Initial temperature, mix proportion, and properties of concrete constituents were input. The prediction models were implemented in the authors' developed computerized program to obtain temperature of concrete in adiabatic conditions. The models included quantitative estimation of degree of reactions, free water content, specific heat, and thermal conductivity. The heat generation obtained from the adiabatic condition was subsequently used as the input in the model to predict semi-adiabatic temperature of mass concrete. The Finite Element Method (FEM) was used to analyze the semi-adiabatic temperature. Dimension of structures, environmental and boundary conditions were input. By the use of the heat transfer analysis with the calculated heat of hydration and thermal properties, the semi-adiabatic temperature distribution in the mass concrete can be analyzed. The details of the prediction models were explained in previous studies [10-15].

### 3.4 Water-soluble sulfate in soils

In order to verify the risk of external sulfate attack, sulfate content of soil samples near the investigated concrete structures was determined. The soil samples were collected at 100 cm deep from ground surface, which was at the same level of bottom faces of the structures. The water-soluble sulfate in soil was determined conforming to ASTM C1580 [16].

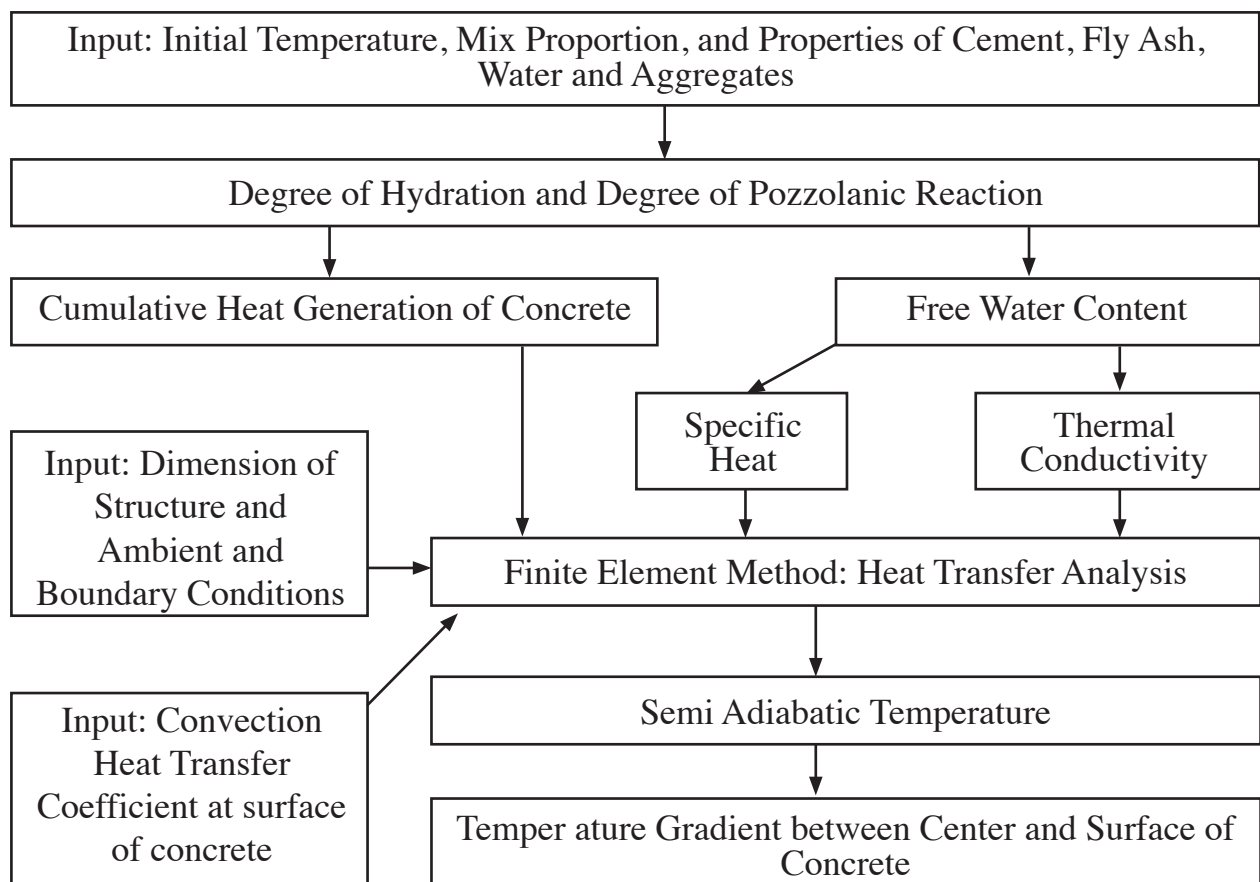


Fig. 3. Flow chart of the models for predicting semi-adiabatic temperature rise of mass concrete.

## 4. Results and discussion

### 4.1 Residual expansion of cored concrete

Fig. 4 shows the residual expansion of cored concrete samples. Cores from structure C (Moderate) showed an expansion of 0.16% at 56 days of exposure while that of structure B (Severe) was 0.14%. The residual expansion of concrete structures A (Very severe) and D (None) were 0.10% and 0.11%, respectively. It can be seen that the cored concrete from structure C (Moderate) had the highest residual expansion which implied a potential for further expansion due to ASR and DEF. The residual expansion of these concrete specimens will be further monitored. The reason why A (Very severe) and B (Severe) show smaller potential expansion when compared to C (Moderate) is that the age of the structures are already longer than 10 years, so the majority of the chemical processes of ASR and DEF had already proceeded before the test. Low potential expansion of D (None) implies that the specimen may have low or no ASR and DEF potentials. D (None) represents the samples with no visible crack on the surface but it does not mean that there is no ASR or DEF in the samples.

### 4.2 Scanning electron microscopy with back-scatter electron mode (SEM/ BSE) and x-ray energy dispersive spectroscopy (EDX) for investigating ASR products and ettringite

The microscopic examination by SEM/BSE with EDX analysis of cored concrete samples at depths of 30 cm and 100 cm was conducted. The microscopic examination of cored concrete samples at 30-cm depth was carried out to identify DEF and ASR products, while that of the samples at 100-cm depth was used to distinguish the formation of ettringite due to external sulfate attack. If the formation of ettringite was caused by external sulfate attack, there should be smaller content of ettringite found in the concrete sample at 100-cm depth than that at 30-cm depth [17]. This is based on the assumption that sulfate solution from the environment can hardly penetrate up to a depth of 100 cm.

The SEM/BSE with EDX analysis of cored concrete samples at a depth of 30 cm revealed that ASR gel and ettringite were found in all concrete samples. For concrete sample A (Very severe), ASR gel was found in paste around aggregate particles, as shown in Fig. 5. Figs. 6 to 9 show examples of ettringite in concrete sample A (Very severe). Fig. 6 shows ettringite-filled interphase gap between paste and aggregate. Cracks through the paste contained a large deposit of ettringite as shown in Fig. 7. The formation of ettringite can be observed in voids and cracks in the aggregate, as shown in Figs. 8 and 9, respectively.

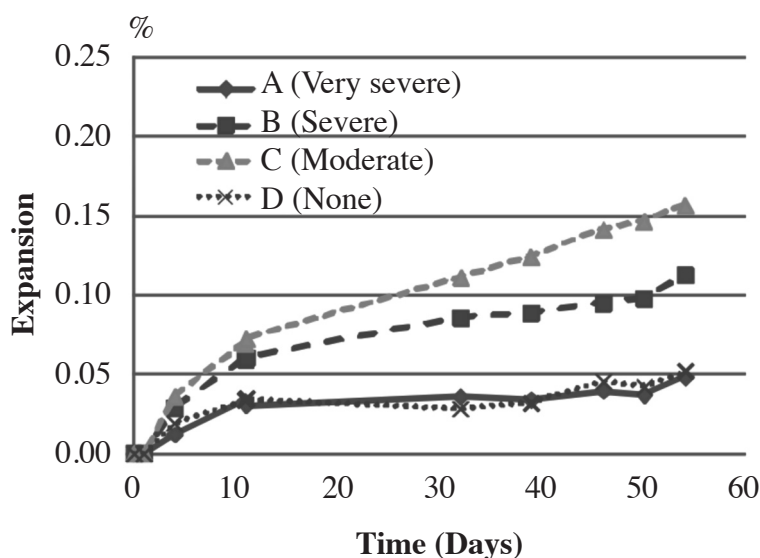
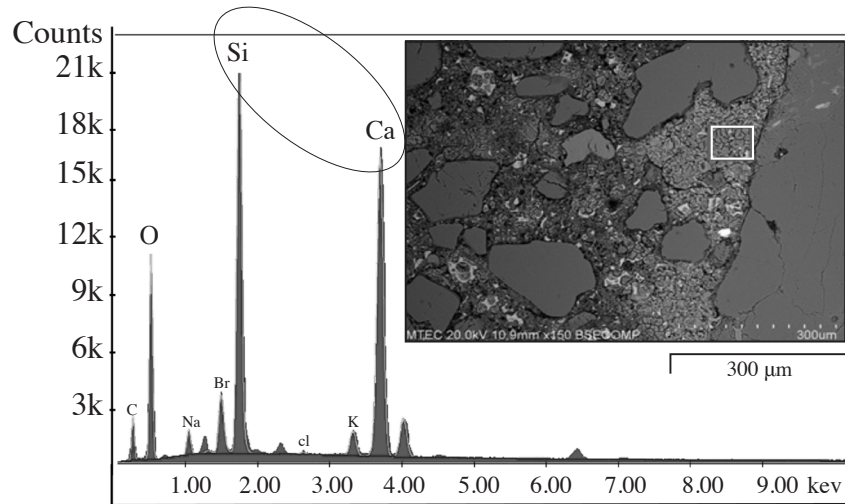
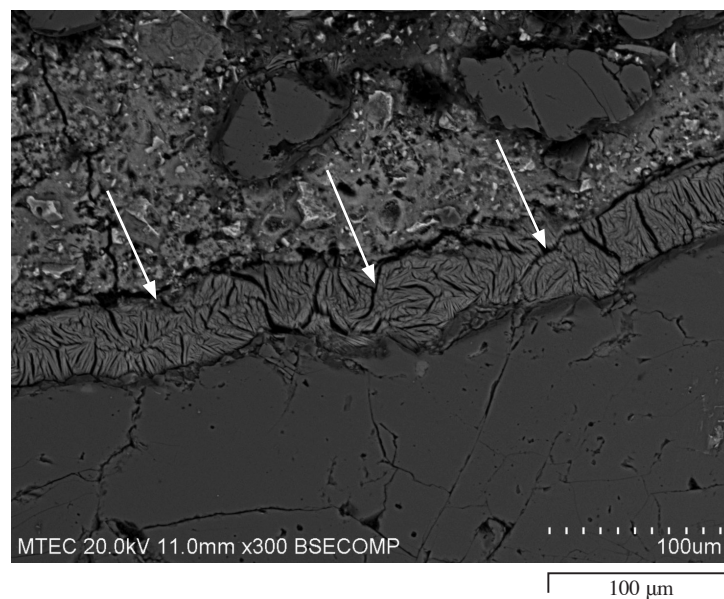


Fig. 4. Residual expansion of cored concrete samples.

ASR gel and ettringite were also detected in other concrete samples. For sample B (Severe), a large deposit of crystallized gel and rosette morphology of ASR gel were found in cracked aggregate as shown in Fig. 10. This rosette-like ASR gel corresponds to the result of Lu et al. [18]. Fig. 11 shows the formation of ASR gel near coarse aggregate and in paste of concrete sample C (Moderate). Fig. 12 shows the ettringite deposit in an interphase gap between paste and aggregate of concrete sample D (None).



**Fig. 5.** BSE image and EDX analysis of concrete sample A (Very severe), showing the formation of ASR gel in paste and its EDX of the intensity of silicon (S) is higher than that of calcium (Ca).



**Fig. 6.** BSE image of concrete sample A (Very severe), showing ettringite-filled interphase gap between paste and aggregate.

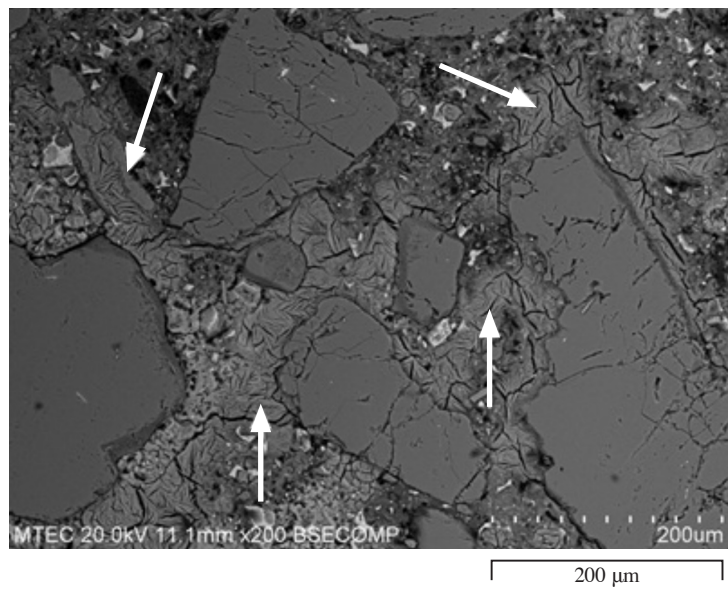


**Fig. 7.** BSE image of concrete sample A (Very severe), showing ettringite filled in cracks, in paste.

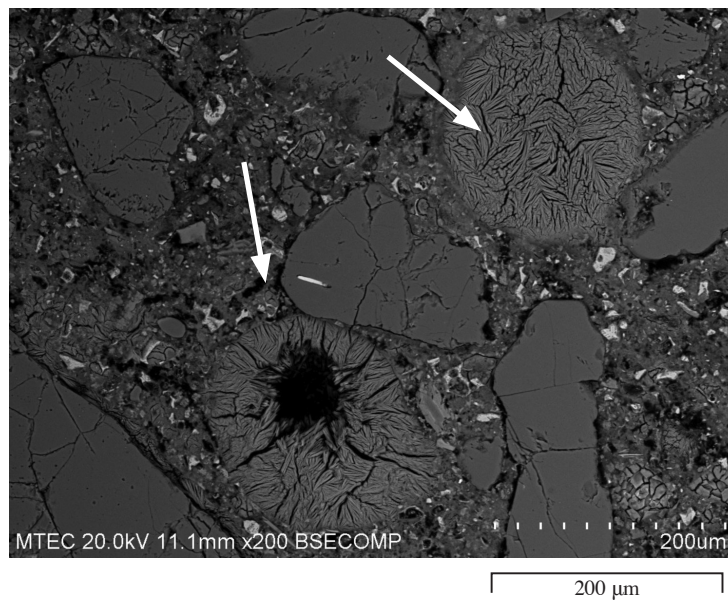


**Fig. 8.** BSE image of concrete sample A (Very severe), showing ettringite filled in voids.

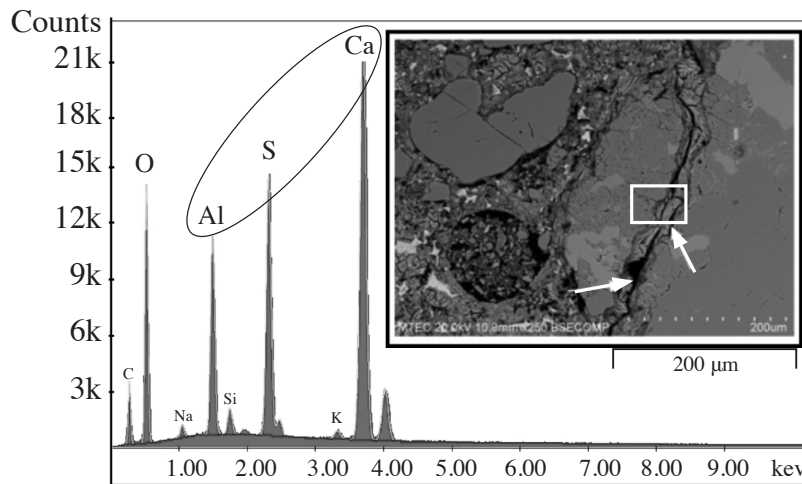


**Fig. 9.** BSE image and EDX analysis of concrete sample A (Very severe), showing cracked aggregate filled with ettringite, and its EDX shows aluminium (Al), sulfur (S) and calcium (Ca).

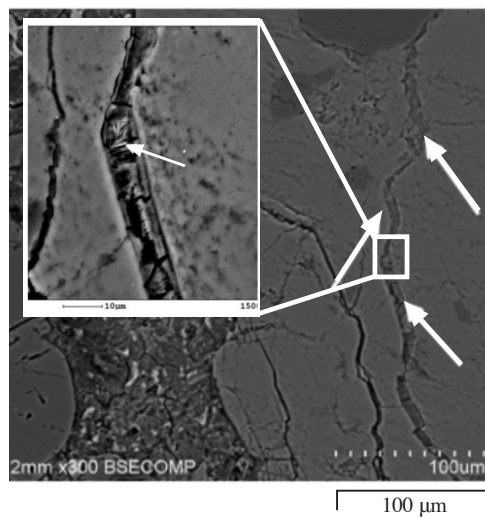


**Fig. 10.** BSE image of concrete sample B (Severe), showing ASR gel in cracked aggregate, with rosette morphology.

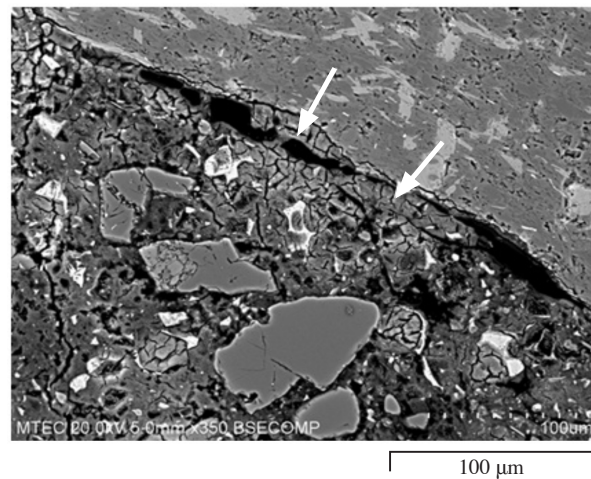


**Fig. 11.** BSE image of concrete sample C (Moderate), showing ASR gel near coarse aggregate and in paste.

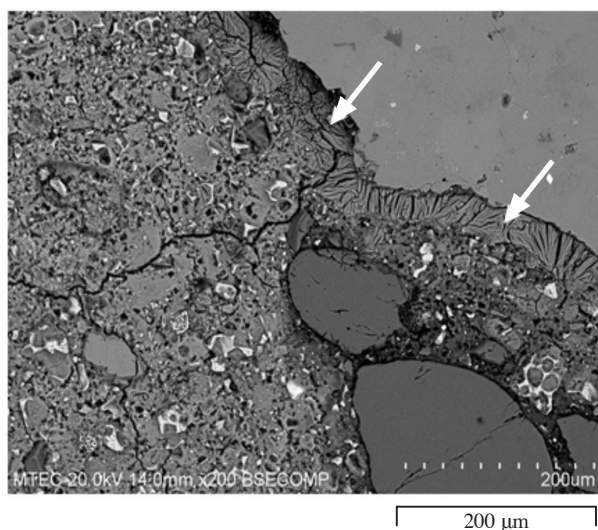


**Fig. 12.** BSE image of concrete sample D (None), showing ettringite-filled interphase gap around aggregate.

For cored concrete samples taken from concrete structures at 100-cm depth, the existence of ettringite was detected in all four samples, whereas the evidence of ASR was only found in samples A (Very severe), B (Severe), and C (Moderate). Location and morphology of ettringite and ASR products found in these samples were similar to that in samples taken from cored concrete at a depth of 30 cm. Moreover, the connectivity of ASR gel and ettringite near aggregate was found in samples taken from concrete structures at 100-cm depth. Fig. 13 shows the formation of ASR gel “I” and ettringite “II” near coarse aggregate in sample C (Moderate). The SEM-EDX elemental mapping analysis of sample B (Severe) (Fig. 14) shows that ASR gel (high intensity of silicon and calcium at “III” and “IV”, respectively) fills in the crack in the aggregate and then extends into the surrounding paste. The extended ASR gel is connected with the vein of ettringite within a gap between the coarse aggregate and the paste. The ettringite is represented by the high intensity of calcium, aluminium, and sulfur at “V”, “VI”, and “VII”, respectively.

The SEM/BSE with EDX analysis of cored concrete samples revealed that ASR gel and ettringite existed in all concrete samples, except in concrete sample D at 100-cm depth. The ASR gel and ettringite were found in many locations such as at the rim around aggregates, in voids and in cracks of paste and aggregates. Table 1 presents a summary of the findings from the SEM/BSE with EDX analysis. The rating was judged by authors based on the amount of ASR gel and ettringite observed in various locations of samples from SEM images. It can be seen that the amounts of ASR gel and ettringite correspond to the damage levels of the concrete structures in the field. The ASR gel and ettringite were mostly found in concrete A which exhibited very severe damage.

The observed existence of ASR gel confirmed that ASR is one of the causes of this concrete deterioration. In the case of DEF, the formation of ettringite could be attributed to either each or a combination of DEF and external sulfate attack. The formation of ettringite in cored concrete samples taken from concrete structures at 100 cm depth supported the occurrence of DEF. Since the amount of ettringite found at 30 cm depth was not higher than those found at 100 cm depth (see Table 1), the internal DEF has a higher potential than the external sulfate attack, and is one of the distress mechanisms. However, confirmation by analyzing the semi-adiabatic temperature rise of concrete and determining sulfate content in soils is to be done in the following sections.

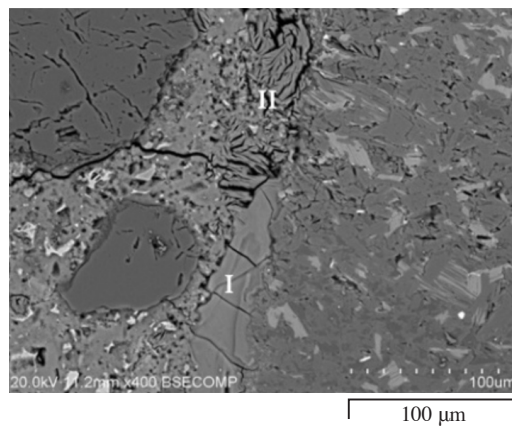


**Fig. 13.** ASR gel “I” and ettringite “II”.

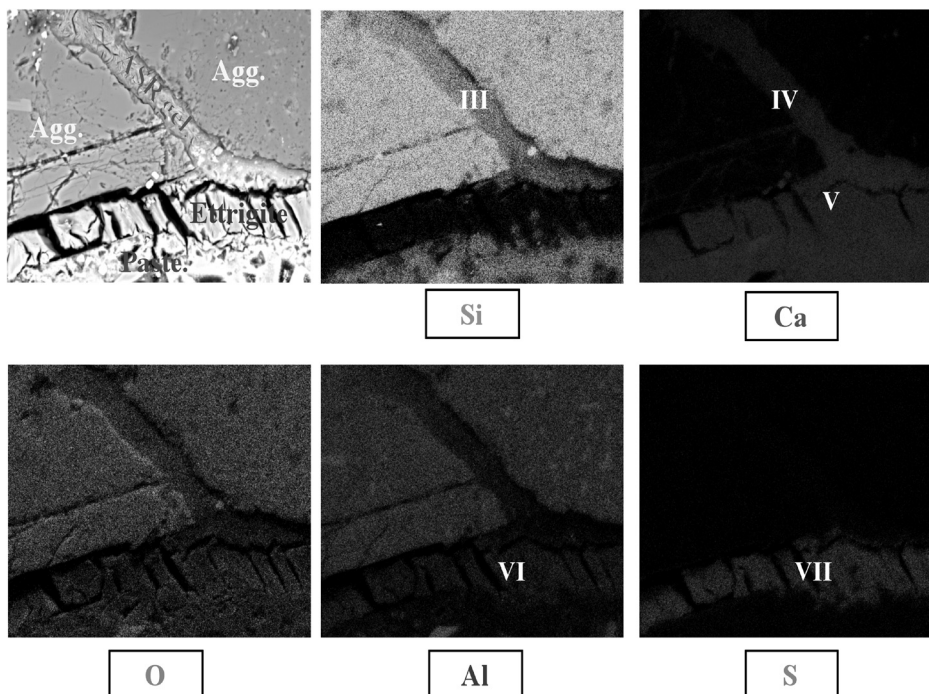


**Fig. 14.** SEM-EDX elemental mapping of ASR gel and ettringite.

**Table 1** Summary on formation of ASR product and ettringite in concrete structures.

Structure	Level of damage	ASR product		Ettringite	
		30 cm.	100 cm.	30 cm.	100 cm.
A	Very severe	****	*	****	****
B	Severe	***	*	**	****
C	Moderate	**	**	***	***
D	None	*	-	**	*

Note: \*\*\*\*= Most,..., \*= Least

### 4.3 Simulation of semi-adiabatic temperature rise of concrete

Semi-adiabatic temperature rise of mass concrete was simulated to confirm the possibility of DEF. A mix proportion of concrete consisting of 294 kg/m<sup>3</sup> of cement, 150 kg/m<sup>3</sup> of water, 860 kg/m<sup>3</sup> of sand, and 1123 kg/m<sup>3</sup> of coarse aggregate, was used in the analysis. From the petrographic analysis, it was found that concrete mixtures were made of different types of aggregate, as shown in Table 2. Two main types of aggregate were granite and limestone. Thermal properties such as specific heat and thermal conductivity of these aggregates are different. Therefore, the simulation of semi-adiabatic temperature rise of mass concrete was conducted on two concrete structures, i.e., A (Very severe) made with granite, and D (None) made with limestone. Thermal coefficients of the aggregates are listed in Table 3. The initial concrete temperatures of 25°C, 37°C, and 42°C were used in the analysis.

Fig. 15 shows the result of analysis of temperature of the mass concrete by using FEM. The simulated semi-adiabatic temperature rise with initial concrete temperatures of 37°C of concrete structures A (Very severe) and D (None) are shown in Figs. 16 and 17, respectively. It can be seen that the temperatures at mid-depth of both cases were over 70°C. Moreover, if the initial temperature of concrete exceeded 35°C, the maximum temperature of the concrete was above 70°C (see Fig. 18). With this concrete temperature at very early age, it is possible for the concrete to encounter DEF [21].

**Table 2** Types of aggregate in concrete structures [19].

Structure	Level of damage	Type of aggregate	
		Coarse aggregate	Fine aggregate
A	Very severe	Granite Mylonite	Granite
B	Severe	Granite Mylonite	Granite
C	Moderate	Granite Mylonite, Politic Hornfels, Limestone, Chert	Granite
D	None	Limestone	Granite

**Table 3** Thermal coefficients of aggregates [20].

Types of coarse aggregate	Limestone	Granite
Specific heat, c (kcal/kg°C)	0.207	0.202
Thermal conductivity, k (kcal/m hr°C)	2.11	2.24

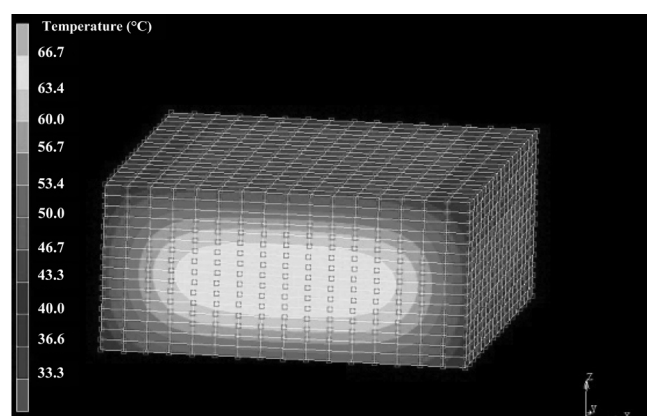


**Fig. 15.** Result of analysis of temperature of mass concrete.

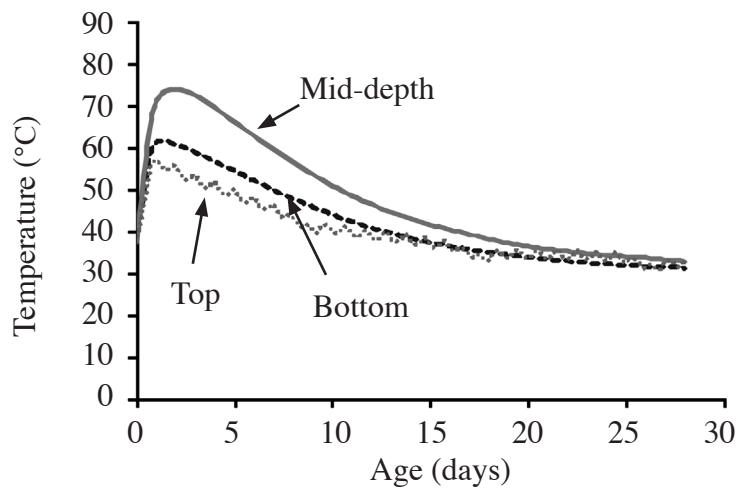


**Fig. 16.** Analytical result of concrete structure A (Very severe).

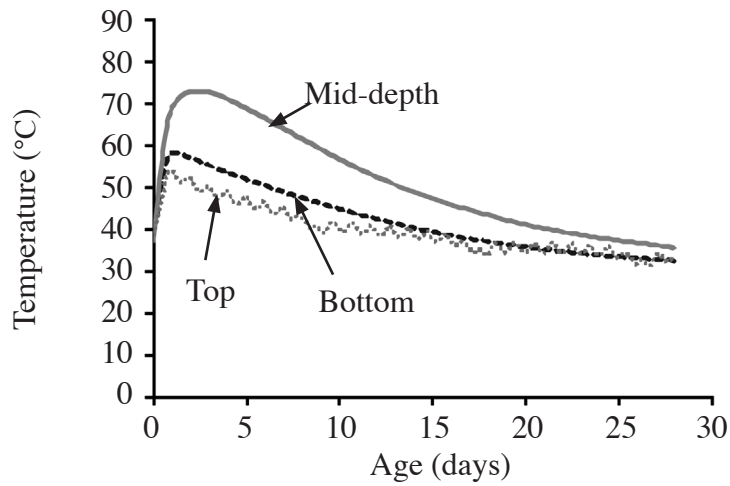


**Fig. 17.** Analytical result of concrete structure D (None).

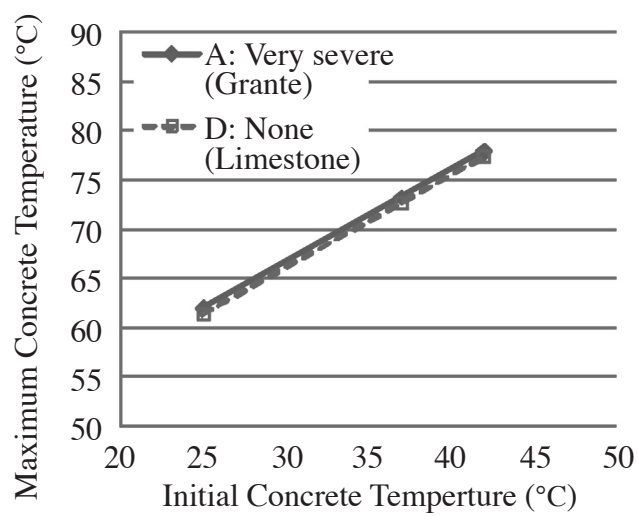


**Fig. 18.** The simulated semi-adiabatic temperature rise of concrete structures.

#### 4.4 Water-Soluble Sulfate in Soils

As another means to investigate the possibility of external sulfate attack, which also forms ettringite in the paste similar to DEF, sulfate content in soil samples near the investigated concrete structures was also determined conforming to ASTM C1580. The amount of water-soluble sulfate in soils near concrete structures A, B, C, and D were 0.08, 0.18, 0.75, and 0.12%, respectively. According to DPT 1332-55 [22] for concrete exposed to sulfate attack, the amount of sulfate in soil near concrete structure A (Very severe) was considered as “Negligible” for severity of sulfate exposure. Soils near concrete structures B (Severe) and D (None) were considered as “Moderate” for severity of sulfate exposure. While Soil near concrete structure C (Moderate) can be considered as “Severe” for severity of sulfate exposure, which provided high risk of external sulfate attack to the concrete structures.

However, the external sulfate attack may not be the cause of damage of the investigated concrete structures in this study since the amount of sulfate in soil was not correlated with the level of damage of the concrete structures. Moreover, cracks were much more observed in concrete above ground level than underground.

#### 5. Conclusions

ASR products and ettringite were observed in many locations of concrete samples such as at the rim around aggregates, in voids and in cracks of paste and aggregates, by using microscopic examination. The amount of ettringite and ASR products was consistent with the damaged levels of the concrete structures. The evidence of ettringite at 100-cm depth were compared with that at 30-cm depth. The analytical results of semi-adiabatic temperature rise in mass concrete, which could increase over 70°C, supported the possible occurrence of DEF. The formation of ettringite was considered to be not involved with the external sulfate attack. All investigated results confirm that ASR and DEF are two of the main causes of cracks in the investigated mass concrete structures.

#### Acknowledgement

The authors would like to acknowledge the research support from the Construction and Maintenance Technology Research Center (CONTEC), the Higher Education Research Promotion and National Research University Project of Thailand, Office of the Higher Education Commission, and National Science and Technology Development Agency (NSTDA).

#### References

- [1] Chatterji S., “Chemistry of alkali-silica reaction and testing of aggregates”, *Cement and Concrete Composites*, Vol. 27, pp. 788-795, 2005.
- [2] Peterson K., et al., “Crystallized alkali-silica gel in concrete from the late 1890s”, *Cement and Concrete Research*, Vol. 36, No. 8, pp. 1523-1532, 2006.
- [3] Fernandes I., et al., “Microscopic analysis of alkali-aggregate reaction products in a 50-year-old concrete”, *Materials Characterization*, Vol. 53, pp. 295-306, 2004.
- [4] Michael Thomas T.R., “Diagnosing the cause of deterioration in prestressed concrete beams-ASR or DEF?”, *Proceeding of the 8<sup>th</sup> Euroseminar on Microscopy Applied to Building Materials*, 2002.
- [5] Stark, J., Bollmann, K., “Delayed ettringite formation in concrete”. In *Proceedings of XVII Symposium on Nordic Concrete Research*, pp. 4-28, 1999.
- [6] Livingston R.A., “Field survey of delayed ettringite formation-related damage in concrete bridges in the State of Maryland”, *American Concrete Institute (ACI)*, pp. 251-268, 2006.
- [7] Thomas M., et al., “Diagnosing delayed ettringite formation in concrete structures”, *Cement and Concrete Research*, Vol. 38, No. 6, pp. 841-847, 2008.

- [8] Natesaiyer K.C. and Hover K.C., "Further study of an in-situ identification method for alkali-silica reaction products in concrete", *Cement and Concrete Research*, Vol. 19, No. 5, pp. 770-778, 1989.
- [9] ASTM 1293. Standard Test Method for Concrete Aggregates by Determination of Length Change of Concrete due to Alkali-Silica Reaction, in *Annual Book of ASTM Standard*, Section 4, 2001.
- [10] Saengsoy W. and Tangtermsirikul S., "Model for predicting temperature of mass concrete", *Proceeding of the 1st National Concrete Conference*, Engineering Institute of Thailand, Kanchanaburi, pp. 211-218, 2003.
- [11] Choktaweekarn P. and Saengsoy W. and Tangtermsirikul S., "A model for predicting thermal conductivity of concrete", *Magazine of Concrete Research*, Vol. 61, No. 4, pp. 271-280, 2009.
- [12] Choktaweekarn P. and Tangtermsirikul S., "Predicting thermal conductivity of concrete", *Proceeding of The Second Asian Concrete Federation Conference*, Bali, Indonesia, pp. CMT 228-CMT 237, November 2006.
- [13] Choktaweekarn P. and Tangtermsirikul S., "Thermal expansion coefficient of concrete", *Proceeding of the 10<sup>th</sup> East Asia Pacific Conference on Structural Engineering and Construction (EASEC-10)*, Bangkok, Thailand, pp. 561-566, August 2006.
- [14] Choktaweekarn P. and Tangtermsirikul S., "Thermal Expansion Coefficient of Cementitious Paste", *ScienceAsia*, Vol. 35, No. 1, pp. 57-63, 2009.
- [15] Choktaweekarn P. and Tangtermsirikul S., "Effect of aggregate type, casting, thickness and curing condition on restrained strain of mass concrete", *Songklanakarin Journal of Science and Technology*, Vol. 32, No. 4, pp. 391-402, 2010.
- [16] ASTM 1580. Standard Test Method for Water-Soluble Sulfate in Soil, *Annual Book of ASTM Standards*, 2009.
- [17] El-Hachem R., Rozière E., Grondin F., Loukili A., "Multi-criteria analysis of the mechanism of degradation of Portland cement based mortars exposed to external sulphate attack". *Cement and Concrete Research* 42, pp. 1327-1335, 2012.
- [18] Lu D., et al., "Alteration of alkali reactive aggregates autoclaved in different alkali solutions and application to alkali-aggregate reaction in concrete: (I) Alteration of alkali reactive aggregates in alkali solutions", *Cement and Concrete Research*, Vol. 36, No. 6, pp. 1176-1190, 2006.
- [19] Yamada K., "ASR problems in Japan", In *Proceeding of the 7<sup>th</sup> Annual Concrete Conference*, Rayong, pp. Keynote-26 - Keynote-35, October 2011.
- [20] Klieger, P., Lamond, J.F., "Significance of tests and properties of concrete and concrete-making materials", 4<sup>th</sup> edn, ASTM Publication, Pennsylvania, 1994.
- [21] Folliard, K., Bauer, S. et al. (2006), "Alkali-Silica Reaction and Delayed Ettringite Formation in Concrete: A literature Review," University of Texas, Center for Transportation Research, CTR 4085-1.
- [22] DPT 1332-55. Standard for durability and service life design of concrete structures, Department of Public Works and Town & Country Planning, 2012.